3662 *Chem. Mater.* **2009,** *21,* 3662–3667
DOI:10.1021/cm900775w

CHEMISTRY OF MATERIALS
Article

Interfacing Metal Nanoparticles with Semiconductor Nanowires

Ilan Jen-La Plante,[‡,§] Susan E. Habas,[†,‡] Benjamin D. Yuhas,[§] Daniel J. Gargas,[§] and Taleb Mokari*[,†,‡]

[†]*The Molecular Foundry and* [‡]*Materials Sciences Division, Lawrence Berkeley National Laboratory and* [§]*Department of Chemistry, University of California at Berkeley, Berkeley, California 94720*

Received March 19, 2009. Revised Manuscript Received May 28, 2009

We demonstrate the overgrowth of Au on CdSe nanowires with control over Au crystal morphology upon increasing addition of Au precursor. Extending this overgrowth technique to catalytically active metals and binary metal systems (Pt, PtCo, and PtNi) exemplifies the broader range of these metal−semiconductor hybrid nanomaterials. Structural and compositional characterization was carried out by low- and high-resolution TEM, EDS analysis, and XRD. Magnetic characterization of the PtCo binary metal hybrid systems was conducted using SQUID magnetometry. Changes in the optical properties of the decorated materials compared to the as-made CdSe nanowires confirm the presence of electronic coupling at the metal−semiconductor interface, an important material property for photocatalytic applications.

Introduction

Recently, there has been significant interest in the design and synthesis of multimaterial, hybrid nanostructures.[1,2] These complex structures incorporate two or more types of materials, an example of which is the formation of metal−semiconductor hybrids, which effectively combine the properties of both materials.[3−8] The rational design of such heterostructures can lead to novel functionalities that are independent of the individual components and may be tailored to fit a specific application. A pressing example of such an application for these hybrid nanostructures is the development of new photocatalytic materials for energy applications.[9] For metal−semiconductor hybrid materials, depending on the electronic alignment of the materials, interactions at the metal−semiconductor interface can facilitate charge separation in the semiconductor or energy transfer between the two materials. The combination of catalytically active metals with semiconductor nanowires that absorb strongly in the visible region of the solar spectrum may show promise as good materials for renewable energy conversion, specifically for photoelectrochemical based cells.

Research in the field of metal−semiconductor nanomaterials has focused on the selective growth of noble metals on the tips of rod and tetrapod semiconductor morphologies.[3,10−14] This architecture lends itself well to forming electrical contacts with the semiconductor.[15,16] In the case of a one-dimensional system, the greater surface area along the length creates a larger number of sites for metal nucleation and growth leading to the formation of high-surface-area materials with multiple reactive sites for photocatalysis. Previous reports involving the incorporation of a secondary material with one-dimensional systems have often employed decoration schemes that rely on physical adsorption or covalent linkage with bifunctional molecules. Hybrid materials prepared via direct attachment are less prevalent, although Weller and co-workers have recently demonstrated the attachment of semiconductor nanoparticles to carbon nanotubes[17] and Talapin and co-workers the direct growth of Au on PbS nanowires.[5] These types of materials are advantageous for

*Corresponding author. E-mail: tmokari@lbl.gov.

(1) Cozzoli, P. D.; Pellegrino, T.; Manna, L. *Chem. Soc. Rev.* **2006**, *35*, 1195.
(2) Shi, W.; Zeng, H.; Sahoo, Y.; Ohulchanskyy, T. Y.; Ding, Y.; Wang, Z. L.; Swihart, M.; Prasad, P. N. *Nano Lett.* **2006**, *6*, 875.
(3) Mokari, T.; Rothenberg, E.; Popov, I.; Costi, R.; Banin, U. *Science* **2004**, *304*, 1787.
(4) Mokari, T.; Sztrum, C. G.; Salant, A.; Rabani, E.; Banin, U. *Nat. Mater.* **2005**, *4*, 855.
(5) Talapin, D. V.; Yu, H.; Shevchenko, E. V.; Lobo, A.; Murray, C. B. *J. Phys. Chem. C* **2007**, *111*, 14049.
(6) Yang, J.; Elim, H. I.; Zhang, Q.; Lee, J. Y.; Ji, W. *J. Am. Chem. Soc.* **2006**, *128*, 11921.
(7) Subramanian, V.; Wolf, E. E.; Kamat, P. V. *J. Phys. Chem. B* **2003**, *107*, 7479.
(8) Kamat, P. V.; Flumiani, M.; Dawson, A. *Colloids Surf., A* **2002**, *202*, 269.
(9) Duonghong, D.; Borgarello, E.; Grätzel, M. *J. Am. Chem. Soc.* **1981**, *103*, 4685.
(10) Habas, S. E.; Yang, P.; Mokari, T. *J. Am. Chem. Soc.* **2008**, *130*, 3294.
(11) Saunders, A. E.; Popov, I.; Banin, U. *J. Phys. Chem. B* **2006**, *110*, 25421.
(12) Pacholski, C.; Kornowski, A.; Weller, H. *Angew. Chem., Int. Ed.* **2004**, *43*, 4774.
(13) Buonsanti, R.; Grillo, V.; Carlino, E.; Giannini, C.; Curri, M. L.; Innocenti, C.; Sangregorio, C.; Achterhold, K.; Parak, F. G.; Agostiano, A.; Cozzoli, P. D. *J. Am. Chem. Soc.* **2006**, *128*, 16953.
(14) Casavola, M.; Grillo, V.; Carlino, E.; Giannini, C.; Gozzo, F.; Fernandez Pinel, E.; Garcia, M. A.; Manna, L.; Cingolani, R.; Cozzoli, P. D. *Nano Lett.* **2007**, *7*, 1386.
(15) Steiner, D.; Mokari, T.; Banin, U.; Millo, O. *Phys. Rev. Lett.* **2005**, *95*, 056805.
(16) Cui, Y.; Banin, U.; Bjork, M. T.; Alivisatos, A. P. *Nano Lett.* **2005**, *5*, 1519.
(17) Juárez, B. H.; Klinke, C.; Kornowski, A.; Weller, H. *Nano Lett.* **2007**, *7*, 3564.

 Published on Web 07/07/2009

applications which require an atomic interface between the components. One-dimensional morphologies also lend themselves to charge transport, an important factor to consider for photocatalytic applications.[18−20] Furthermore, a hybrid metal−semiconductor nanowire may demonstrate increased conductivity due to the influence of the metallic overgrowth. Interactions between the electronic states of the metal with those of the semiconductor can lead to changes in the local density of states and enhanced charge separation in the semiconductor material due to energy band alignment. Engineering of such properties is crucial for the rational design and synthesis of new classes of photocatalytic materials.

Here, we demonstrate the synthesis of metal−semiconductor hybrid nanowires via metal overgrowth onto solution−liquid−solid (SLS) grown nanowires. The systems developed include metal (Au, Pt) and binary metal (PtNi, PtCo) hybrids with CdSe nanowires. Metal overgrowth on the nanowires is achieved by reducing a metal salt in the presence of the semiconductor nanowires. We note changes in the morphology of the decorative growth as the concentration of metal precursor is altered. Optical characterization of the nanowires before and after overgrowth support strong electronic coupling at the metal−semiconductor interface as we reported previously.[3] As novel multifunctional hybrid nanomaterials, these structures are very interesting for a variety of applications, including the photocatalytic generation of hydrogen from water.

Experimental Section

CdSe Nanowire Synthesis. CdSe nanowires were grown by a previously reported form[21] of the SLS growth mechanism.[22] Briefly, cadmium oxide (CdO 99.99%, 0.006 g, 0.047 mmol) was complexed with *n*-tetradecylphosphonic acid (*n*-TDPA 97%, 0.0270 g, 0.097 mmol) in trioctylphosphine oxide (TOPO 99%, 5 g) for 90 min at 300 °C under N_2 using standard Schlenk technique. The catalyst, a 6 nm thin film of Bi, was thermally evaporated on top of a 2.5 nm sticking layer of Cr on a Si(100) substrate. In a typical synthesis, one or two ~0.4 cm^2 Si substrates were added to the Cd-TDPA solution at 270 °C. Since the bulk melting point of Bi is 271 °C, some of the Bi thin film melts and dewets from the surface of the substrate forming Bi nanoparticle catalysts. Next, 0.25 mL of 2.5 wt % selenium (99.5% powder mesh) dissolved in trioctylphosphine (97%) was injected into the solution. After 5 min of growth time, the solution was cooled and then diluted with 5−10 mL of toluene. The CdSe nanowires suspended in solution were precipitated by addition of methanol followed by centrifugation. The product was stored as a colloidal suspension in toluene.

The CdSe wires were decorated with Au according to a method described previously.[3] A toluene solution containing gold trichloride ($AuCl_3$, 12 mg, 0.03 mmol), didodecyldimethylammonium bromide (DDAB, 40 mg, 0.09 mmol), and dodecylamine (DDA, 70 mg, 0.38 mmol) was sonicated for 5 min and then added dropwise to a suspension of nanowires stirring under N_2. The product was precipitated with methanol and separated by centrifugation. The amount of precursor added was varied to give the desired degree of Au overgrowth.

Decoration of the CdSe wires with Pt, PtNi, and PtCo was achieved as described previously.[10] Oleic acid (0.2 mL), oleylamine (0.2 mL), and 1,2-hexadecanediol (43.0 mg) were heated in diphenyl ether (10 mL) at 80 °C under vacuum for 30 min to remove traces of water. Platinum acetylacetonate (32.8 mg) was added to a suspension of CdSe nanowires in 1,2-dichlorobenzene and heated at 65 °C for 10 min to promote dissolution of the Pt precursor. The mixture of surfactants and diphenyl ether was purged with nitrogen and heated to 200 °C before injecting the Pt precursor and semiconductor wires. After several minutes, the reaction was removed from heat and quenched in a water bath. The product was washed by precipitation with ethanol followed by centrifugation. Either nickel or cobalt acetate was added to the reaction prior to heating to 80 °C to promote PtNi or PtCo formation. Control over the binary composition is possible by altering the ratio of the metallic components or by changing the metal to CdSe nanowire ratio.

The structure and composition of the samples were investigated by TEM and HRTEM (Tecnai G2 S-Twin microscope operated at 200 kV and JEOL 2100-F Field-Emission Analytical Transmission Electron Microscope operated at 200 kV), EDS (Philips CM200/FEG microscope operated at 200 kV, equipped with a Link EDS detector, and a Weiss FESEM Ultra-55 operated at 30 kV), and XRD (Bruker-AXS D8 with a general area detector and Co Kα radiation). Samples were dispersed on carbon coated copper grids for TEM or glass substrates for XRD. Toluene suspensions of the nanowires were prepared for analysis by UV−vis absorption spectroscopy (Shimadzu UV-3600), and PL spectroscopy was performed using a 532 nm excitation source for disperse samples on TEM grids. Image correlation for PL measurements was performed using the STEM mode on a Weiss FESEM Ultra-55 operating at 30 kV. Magnetic measurements were performed on powder samples of the PtCo-overgrown CdSe nanowires with a SQUID magnetometer (Quantum Design MPMS XL).

Results and Discussion

Synthesis and Characterization of CdSe Nanowires. Cadmium selenide nanowires grown via the SLS method[23,24] exhibit high aspect ratios due to the fast reaction kinetics, and are both straight and single-crystalline as seen by transmission electron microscopy (TEM) and high-resolution TEM (HRTEM, Figure 1A,B). Measured lattice spacings of 3.5 Å match those of the (002) lattice planes corresponding to growth along the ⟨001⟩ direction. This data is in accordance with previous reports on the crystal structure of SLS-grown CdSe nanowires.[25] As-grown CdSe nanowires have diameters of less than 10 nm and lengths up to 10 μm. The nanowires are monodisperse in diameter, which can be attributed to both the uniform

(18) Dukovic, G.; Merkle, M. G.; Nelson, J. H.; Hughes, S. M.; Alivisatos, A. P. *Adv. Mater.* **2008**, *20*, 4306.
(19) Elmalem, E.; Saunders, A. E.; Costi, R.; Salant, A.; Banin, U. *Adv. Mater.* **2008**, *20*, 4312.
(20) Hsu, Y.-J.; Lu, S.-Y.; Lin, Y.-F. *Chem. Mater.* **2008**, *20*, 2854.
(21) Trentler, T. J.; Hickman, K. M.; Goel, S. C.; Viano, A. M.; Gibbons, P. C.; Buhro, W. E. *Science* **1995**, *270*, 1791.
(22) Ouyang, L.; Maher, K. N.; Yu, C. L.; McCarty, J.; Park, H. *J. Am. Chem. Soc.* **2007**, *129*, 133.
(23) Yu, H.; Li, J.; Loomis, R. A.; Gibbons, P. C.; Wang, L.-W.; Buhro, W. E. *J. Am. Chem. Soc.* **2003**, *125*, 16168.
(24) Grebinski, J. W.; Richter, K. L.; Zhang, J.; Kosel, T. H.; Kuno, M. *J. Phys. Chem. B* **2004**, *108*, 9745.
(25) Grebinski, J. W.; Hull, K. L.; Zhang, J.; Kosel, T. H.; Kuno, M. *Chem. Mater.* **2004**, *16*, 5260.

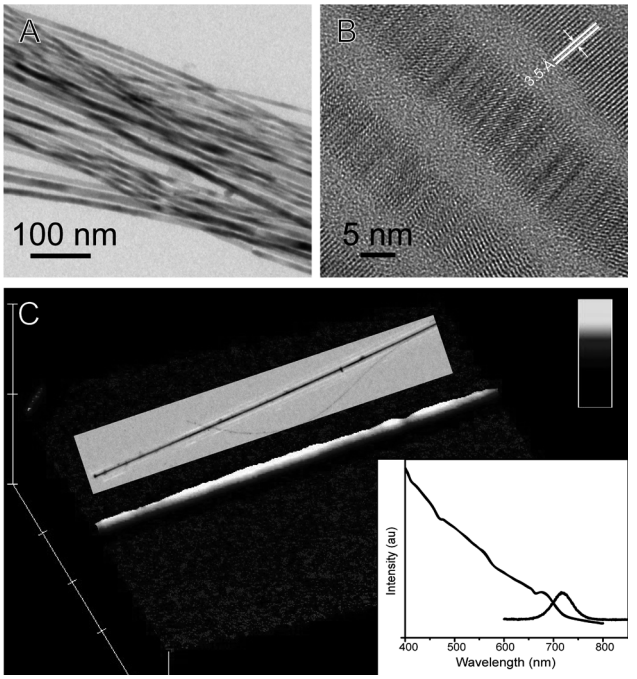

Figure 1. (A) Low- and (B) high-resolution TEM images of CdSe nanowires. (C) Confocal optical microscope image of a single CdSe nanowire correlated with adjacent TEM image of the same wire. Inset shows photoluminescence spectrum showing wire photoluminescence centered at 715 nm.

dewetting of the Bi thin film upon heating and the high stirring rate, leading to a regular distribution of melted Bi droplets in solution.[26] Nanowires produced by this method exhibit photoluminescence (PL) centered at 715 nm (Figure 1C, inset) which is similar to bulk PL (CdSe Bohr exciton radius ~6 nm). Spectra were correlated by confocal microscopy and scanning transmission electron microscopy (STEM) mode scanning electron microscopy (SEM) imaging to ensure that each measurement corresponded to a single wire (Figure 1C).

Overgrowth of CdSe Nanowires with Au. Integration of metallic components with semiconductor nanowires can lead to multifunctional hybrid materials with advanced properties. For example, the formation of metal−semiconductor interfaces could facilitate electrical connection for device fabrication by providing a natural metallic anchor point for electrode wiring. Additionally, growth of metals on semiconductors may lead to an increase of the optical absorbance of the semiconductor nanostructures.[27] Finally, there is also the potential for photoinduced charge separation mediated by alignment of the energy levels of the two materials.

Overgrowth of Au on the CdSe nanowires was achieved by reduction of a gold salt ($AuCl_3$) with dodecylamine in the presence of a surfactant (DDAB). By varying the amount of Au precursor introduced, distinct changes in overgrowth morphology were observed. At low concentrations, Au grows predominantly at the tips of the wires and at relatively few locations along the length of the wire

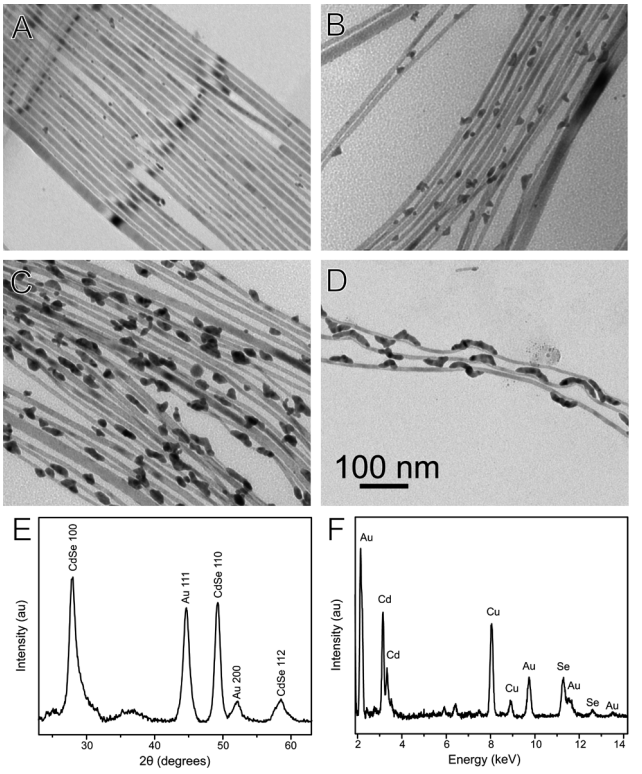

Figure 2. (A−D) Morphology changes of Au overgrowth on CdSe nanowires with increasing addition of Au precursor. (A) The lowest concentration of Au precursor added corresponds with a low concentration of nanoparticle growth along the wire. (D) At the highest level of Au precursor addition, Au growth occurs as extended regions along the nanowire with triangular morphology. Characterization of these materials includes XRD (E) and EDS (F) analysis.

(Figure 2A). This growth is likely an effect of the higher energy at the wire tips and defect sites which agrees with our previous reports for metal overgrowth on CdSe rods and tetrapods, as well as CdS rods. As a result, wires with smaller diameters show higher levels of Au coverage due to the increased surface energy. In longer one-dimensional systems such as high aspect ratio nanowires, the increased surface area along the length of the wire compared to quasi-1D shapes such as rods allows for greater probability of growth on defect lattice sites with higher surface energies.

As the concentration of Au precursor was increased, Au coverage also increased. In addition to a greater degree of Au overgrowth, distinct triangular islands of Au growth were observed (Figure 2B). The morphology of the Au overgrowth at low concentrations resembles discrete gold nanoparticles attached to the CdSe wire, while at increasing concentrations, the Au adopts the shape of triangular islands attached along the wire. For wurtzite lattice CdSe nanowires grown along the ⟨001⟩ direction, the lattice mismatch for Au overgrowth along the faces is large (CdSe hexagonal, $a = 4.299$ Å, $c = 7.01$ Å; Au cubic $a = 4.08$ Å), and the resulting strain is sufficient to induce island-like growth morphologies.

As the addition of Au is increased further, we continue to see triangular island growth with higher coverage. However, upon reaching some critical Au concentration, the growth mode appears to change from discrete island

(26) Wang, Y.; Xia, Y. *Nano Lett.* **2004**, *4*, 2047.
(27) Schaadt, D. M.; Feng, B.; Yu, E. T. *Appl. Phys. Lett.* **2005**, *86*, 063106.

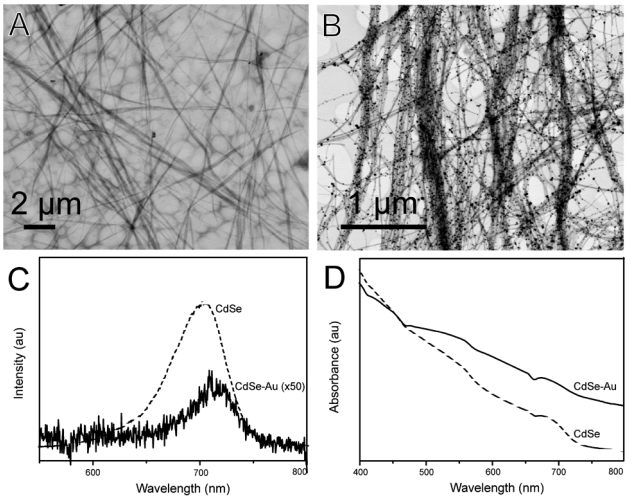

Figure 3. Photoluminescence spectra of CdSe and Au-CdSe nanowires. SEM images using STEM mode detector overview images of (A) CdSe and (B) Au-CdSe nanowires for PL measurements. (C) PL intensity shows marked decrease upon addition of Au overgrowth. Upper trace shows PL spectrum for as-grown CdSe nanowires, lower trace shows PL spectrum multiplied 50 times for the Au-CdSe nanowires. (D) Absorbance spectra before and after decorative growth show broadening of the absorption features following Au addition. Spectra are offset for clarity.

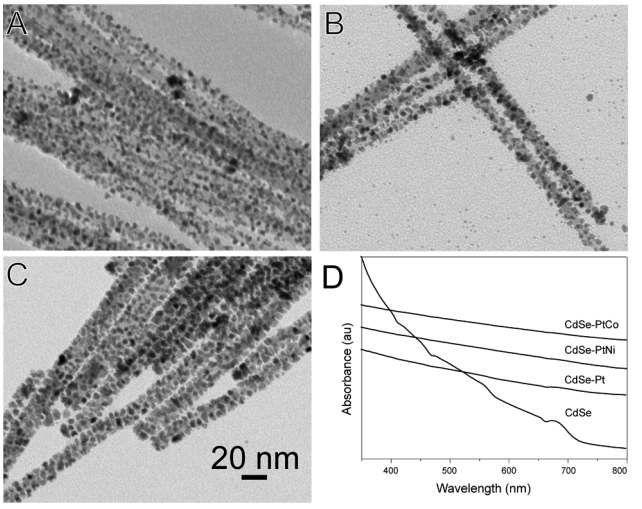

Figure 4. (A) Pt, (B) PtNi, and (C) PtCo growth on CdSe nanowires. (D) UV−vis absorbance spectra for the original CdSe nanowires, Pt-CdSe, PtNi-CdSe, and PtCo-CdSe decorated wires demonstrate broadening of the absorption features of the original CdSe nanowires.

growth to larger areas of continuous Au growth (Figure 2C). Such growth morphologies could occur due to ripening of the Au and reformation at more stable growth points. After the Au concentration increases past this critical point, the areas of continuous Au growth increase in length (Figure 2D). Eventually, the CdSe wire itself begins to bend to accommodate strain from the lattice mismatch of the Au overgrowth. Distortion of the CdSe wire lattice grows more severe with increasing thickness of the Au islands. At the highest Au precursor concentration, we see marked changes in the structural integrity of the CdSe nanowires (see Supporting Information, Figure S1).

Following Au growth, the composition of the materials was characterized by both XRD and EDS analysis. Figure 2E shows an X-ray diffraction pattern with three peaks indexed to the (100), (110), and (112) peaks for bulk wurtzite CdSe. The remaining peaks characteristic of the wurtzite CdSe pattern are not visible because of alignment of the wires on the substrate along the *c*-axis as a result of drying patterns from dropcasting. To visualize the complete diffraction pattern, we also performed XRD on CdSe nanowires grown on a substrate from the same synthetic procedure. These wires exhibited random orientation leading to additional peaks that are indexed to the (002), (101), and so forth wurtzite planes. A second set of peaks can be indexed to the (111) and (200) planes of face-centered cubic (fcc) Au, indicating the crystalline nature of the Au overgrowth. Selected area energy dispersive X-ray spectroscopy (EDS) performed on a region of the Au−CdSe interface confirms the presence of Au (Figure 2F).

Optical Characterization of Au−Semiconductor Hybrid Materials. Changes in the optical properties of the CdSe nanowires upon Au overgrowth suggest that there exists strong electronic coupling between the metal and the semiconductor. Absorbance spectra of the wires were taken before and after Au growth (Figure 3D). In the lower spectrum before Au overgrowth (dotted trace), distinct CdSe absorption features are evident correlating with the first excitonic peak around 680 nm. Following the addition of Au overgrowth (solid trace), the major absorption features occur at the same wavelengths but are broadened markedly, which agrees with our previous report.[3]

Similarly, the electronic coupling between the two materials is manifested in the photoluminescence (PL) properties of the hybrid nanowires. We see significant quenching of the CdSe PL, which could result from energy transfer or electron transfer from the semiconductor to the metal (further study of excited state lifetimes is being carried out at our laboratory to distinguish between the two competitive processes). Bulk PL measurements proved difficult owing to the strong scattering effect of the solution dispersed CdSe nanowires. Instead, TEM grids with the as-grown CdSe and Au-CdSe nanowires were prepared, and grid squares with similar amounts of nanowire coverage were located with SEM images using STEM mode (Figure 3A,B). Excitation at 532 nm over a spot size with the approximate area of a TEM grid square gave the PL spectra shown in Figure 3C for undecorated (dotted trace) and Au-decorated CdSe nanowires (solid trace). PL spectra were correlated to the SEM images shown in Figure 3A,B. As shown earlier by confocal microscopy, the as-grown CdSe nanowires show strong PL centered at 715 nm. However, for the Au-CdSe hybrid system, the PL signal decreased by 2 orders of magnitude.

Metal-CdSe Nanowire Heterostructures as Multifunctional Materials. Overgrowth of Au on CdSe nanowires demonstrates the evolution of new properties from multimaterial heterostructures that are independent of the individual components. Extension of this concept to catalytic and magnetic materials can introduce additional

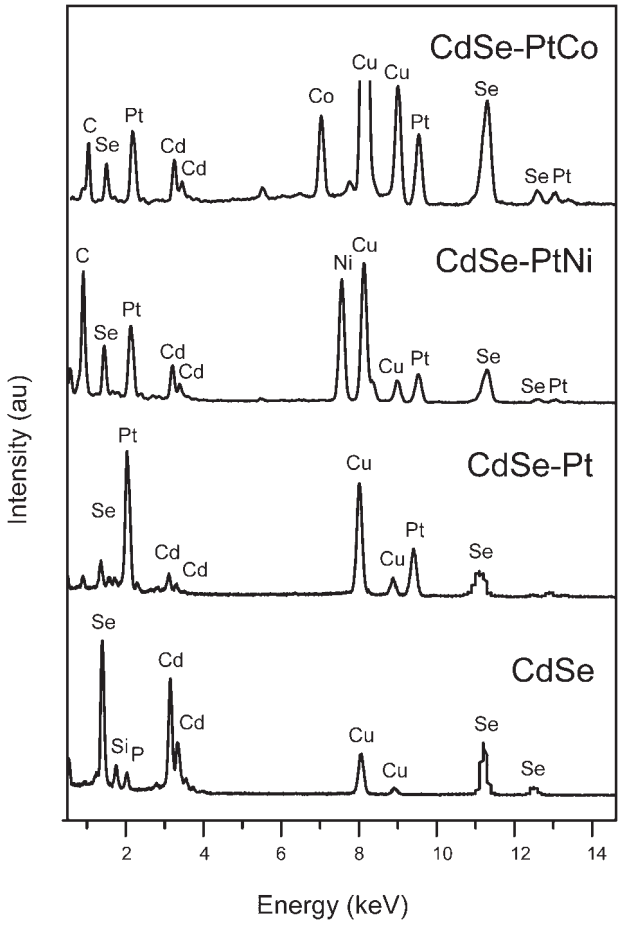

Figure 5. Energy dispersive X-ray spectroscopy (EDS) analysis of as-grown CdSe nanowires, CdSe-Pt, CdSe-PtNi, and CdSe-PtCo systems.

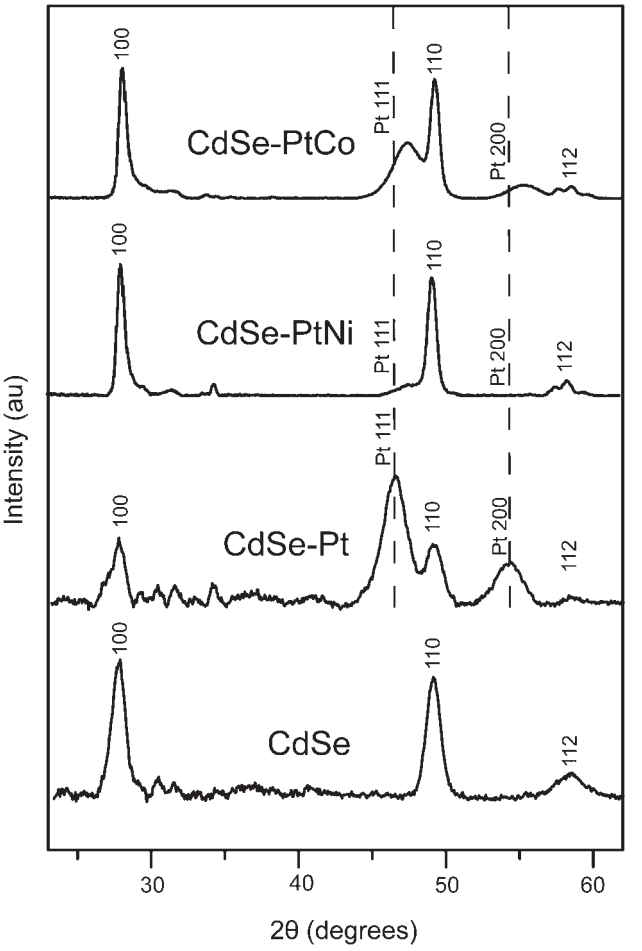

Figure 6. X-ray diffraction patterns for as-grown CdSe nanowires, CdSe-Pt, CdSe-PtNi, and CdSe-PtCo systems. Introduction of the Pt (111) and (200) diffraction peaks confirms the crystalline nature of the metal overgrowth.

properties to create multifunctional heterostructures for photocatalytic and magnetic applications. Nanostructured Pt is a well-known heterogeneous catalyst that is often integrated with a solid support material.[28,29] Incorporation of Pt and binary catalytic materials with a photoactive substrate such as CdSe nanowires introduces the potential for photocatalytic activity. We have expanded upon the Au-CdSe system to include decoration of CdSe nanowires with Pt nanoparticles. A Pt salt was reduced in the presence of CdSe nanowires according to our previously reported procedure.[10] The resulting growth was similar to that seen for the Au decoration at the lowest levels of Au precursor addition; however, overall coverage of the nanowire surface with Pt nanoparticles was much higher (Figure 4A). Although high-density coverage of the semiconductor substrate by Pt nanoparticles is shown here, the coverage can be controlled by changing the amount of added Pt precursor leading to a material coverage which may be optimized for photocatalytic applications. For the Au-CdSe system, higher levels of Au precursor addition yielded larger isolated islands, whereas higher concentrations of added Pt precursor increased the density of overgrowth coverage. The difference in growth coverage can be explained by the differences in reaction conditions. The Au overgrowth reaction is done at room temperature; however, the Pt overgrowth reaction is done at a higher temperature (200 °C) to increase the interaction between the CdSe and Pt. Finally, while there is some variation in the size distribution of the Pt nanoparticles, most are < 5 nm in diameter, a size range shown to be highly active for catalytic reactions such as ethylene hydrogenation.[28]

The introduction of binary metals as a component of the hybrid materials allows for controlled variation of the catalytic and magnetic properties. By incorporating Ni or Co precursors into the Pt growth reaction (Figure 4B,C), we can form binary metal overgrowth with similar morphologies to the Pt case. Such metal combinations expand our library of potential materials for photocatalytic applications. As before with the addition of Au growth to the nanowires, for all three cases (Pt, PtNi, and PtCo) we note a broadening and washing out of the absorption features indicating electronic coupling at the interface and not simply metal decoration on the semiconductor surface. Absorbance spectra for these systems are shown in Figure 4D.

(28) Song, H.; Rioux, R. M.; Hoefelmeyer, J. D.; Komor, R.; Niesz, K.; Grass, M.; Yang, P.; Somorjai, G. A. *J. Am. Chem. Soc.* **2006**, *128*, 3027.
(29) Formo, E.; Lee, E.; Campbell, D.; Xia, Y. *Nano Lett.* **2008**, *8*, 668.

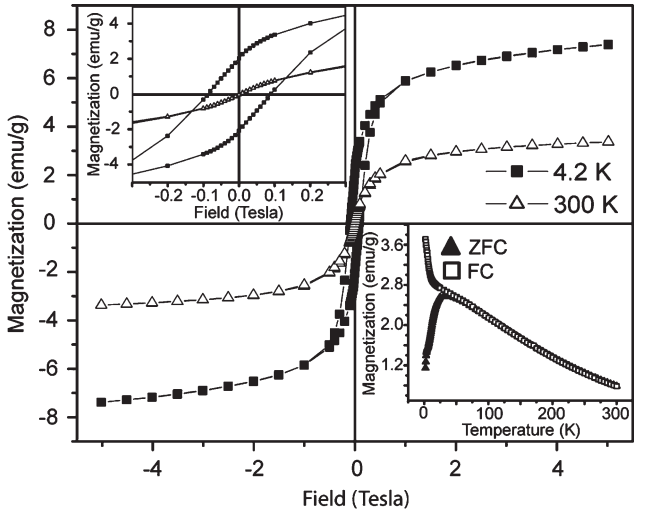

Figure 7. SQUID magnetometry results for PtCo-CdSe hybrid nanowires showing temperature-dependent magnetization measurements. Hysteresis loops are measured at 300 K (triangles) and 4.2 K (squares). Upper inset provides a magnified view of the graph around zero field. Lower inset shows traces of magnetization as a function of temperature in zero-field cooled (triangles) and field-cooled (squares) modes which demonstrates superparamagnetic behavior with a blocking temperature of approximately 30 K.

Compositional characterization of these systems was carried out by EDS and XRD. Figure 5 shows EDS data collected directly on metal growth sites confirming the addition of Pt decoration and incorporation of Ni and Co in the binary metal systems. Peaks corresponding to Cu in all spectra arise due to the Cu TEM grid. Diffraction patterns are provided in Figure 6 for the as-made CdSe nanowires, as well as the Pt-CdSe, PtNi-CdSe, and PtCo-CdSe hybrid structures. The as-made CdSe nanowires exhibit a diffraction pattern corresponding to bulk wurtzite CdSe. Upon Pt overgrowth, two peaks indexed to the (111) and (200) planes of face-centered cubic Pt appear confirming the crystalline nature of the metal decoration. For the binary metal overgrowth of PtNi and PtCo, a shift to higher angle is noted for the Pt (111) and (200) peaks corresponding to a contraction of the Pt lattice due to Ni or Co incorporation.

Magnetic characterization of the PtCo-CdSe hybrid nanowires was performed using SQUID magnetometry. Hysteresis loops are presented for the PtCo-CdSe hybrid nanowires for both 300 and 4.2 K in Figure 7. The lower inset displays temperature-dependent magnetization measurements done in both zero-field cooled and field-cooled modes. The structures exhibit superparamagnetic behavior with a blocking temperature of approximately 30 K, which is typical of nanoscale PtCo particles.[30] We thus see that, in this case, the magnetic properties of the PtCo alloys are preserved upon growth onto the CdSe nanowires. The possibility also could exist that, through some synthetic modifications, hybrid structures with different magnetic properties from the free PtCo NP counterparts could be created, although further study on this subject is currently ongoing.

Conclusions

We have demonstrated the overgrowth of a variety of metals and binary metals onto CdSe nanowires. Structural characterization showed that the morphology of Au decoration varied with increasing amount of Au precursor added. Growth begins with discrete island formations, which then lead to extended areas of growth with increasing Au addition. The development of complementary systems with Pt, PtNi, and PtCo decoration shows the adaptability of this synthetic technique to an array of catalytic and magnetic metals. Electronic coupling between the semiconductor wire and metallic nanoparticles was confirmed by changes in the optical properties of the materials including broadening of the absorption features and quenching of the photoluminescence spectra. Further study is needed to explore the photocatalytic and conductive properties of these multifunctional hybrid materials.

Acknowledgment. Work at the Molecular Foundry was supported by the Director, Office of Science, Office of Basic Energy Sciences, Division of Materials Sciences and Engineering, U.S. Department of Energy, under Contract DE-AC02-05CH11231. We thank Prof. Peidong Yang for useful discussion. We thank Prof. Jeff Long for the use of the SQUID magnetometer.

Supporting Information Available: High-resolution transmission electron microscopy of strained CdSe nanowires following Au growth and X-ray diffraction from nonoriented CdSe nanowires (PDF). This material is available free of charge via the Internet at http://pubs.acs.org.

(30) Wiekhorst, F.; Shevchenko, E.; Weller, H.; Kötzler, J. *Phys. Rev. B* **2003**, *67*, 224416.